

**Supplementary Material for:**

**Adaptive alterations in the mesoaccumbal network following peripheral nerve injury**

Wenjie Ren<sup>1,2</sup>, Maria Virginia Centeno<sup>1,2</sup>, Xuhong Wei<sup>1</sup>, Ian Wickersham<sup>3</sup>, Marco Martina<sup>1,2</sup>, A. Vania Apkarian<sup>1,2</sup> and D. James Surmeier<sup>1,2</sup>

<sup>1</sup>Department of Physiology, Feinberg School of Medicine, Northwestern University, 303 E. Chicago Ave., Chicago, IL 60611

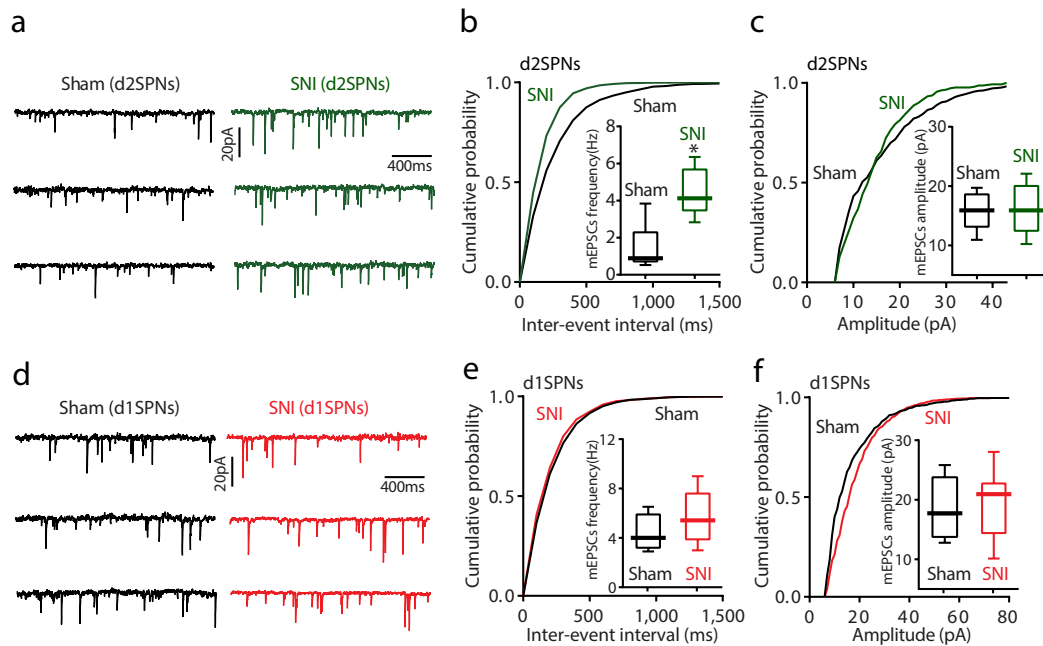
<sup>2</sup>Center of Excellence for Chronic Pain and Drug Abuse Research

<sup>3</sup>McGovern Institute for Brain Research, Massachusetts Institute of Technology, Cambridge, Massachusetts 02139

Six supplementary figures.

## Supplemental Figures

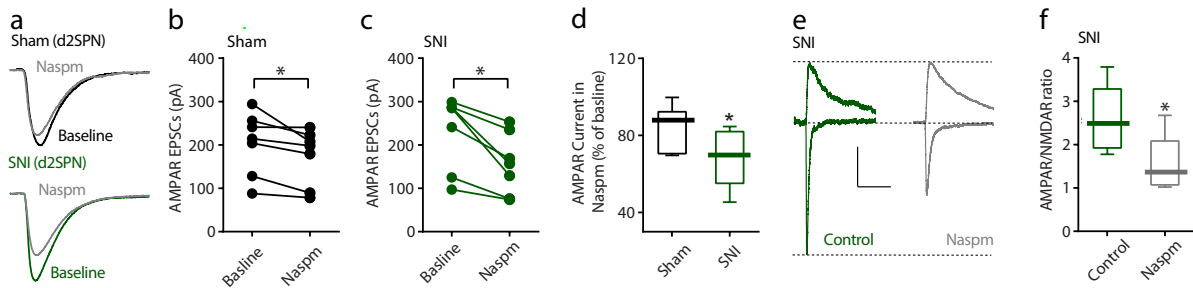
Figure S1 - Ren et al.



**Figure S1. SNI increased synaptic input in cNac d2SPNs but had no effect on cNac d1SPNs.** *a-c*, In SNI, the d2SPN mEPSC frequency was augmented without detectable change in the amplitude of d2SPN mEPSC (n= 6 neurons from 6 mice per group; Kolmogorov-Smirnov test for representative cumulative probability plots with  $D = 0.5000$ ,  $P = 0.0366$  for **b** and  $D = 0.2632$ ,  $p = 0.1439$  for **c**; Mann-Whitney  $U$  test for box plots with  $U = 3$ ,  $P = 0.0152$  for **b** and  $U = 18$ ,  $p > 0.9999$  for **c**). *d-f*, there is no difference in mEPSCs frequency or amplitude of d1SPNs between SNI and Sham animals (n = 8 from 6 mice in each group, Kolmogorov-Smirnov test for representative cumulative probability plots with  $D = 0.1462$ ,  $p = 0.9891$  for **e** and  $D = 0.1600$ ,  $p = 0.2923$  for **f**; Mann-Whitney test for box plots with  $U = 20$ ,  $p = 0.2317$  for **e** and  $U = 29$ ,  $p =$

0.7768 for **f**). Whisker box plots are displayed as median, lower and upper quartiles, and whiskers representing minimum and maximum of the data.

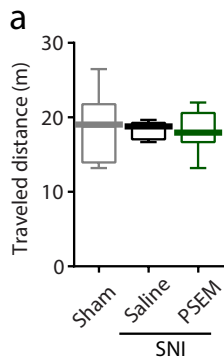
Figure S2 - Ren et al.



**Figure S2. SNI increased the proportion of calcium-permeable AMPARs at PL-cNAc synapses.**

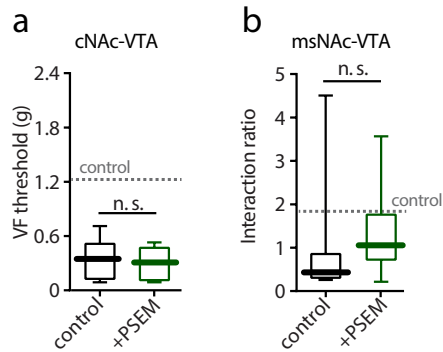
**a-c**, Calcium-permeable AMPAR antagonist Naspm decreased AMPAR EPSC amplitudes in sham and SNI mice ( $n = 7$  neurons from 5 mice per group; Wilcoxon test with  $W = -28$ ,  $p = 0.0156$  for **b**  $W = -28$ ,  $p = 0.0156$  for **c**). **d**, Naspm had bigger effect on the d2SPNs from SNI mice than those from sham mice (Mann-Whitney  $U$  test with  $U = 7$ ,  $p = 0.0262$ ). **e-f**: Naspm reversed enhanced A/N ratio at PL-cNAc d2SPNs synapse in SNI mice ( $n = 6$  neurons from 5 mice per group; Mann-Whitney  $U$  test with  $U = 5$ ,  $p = 0.0411$ ; calibration: 50 pA, 100 ms). Data are presented as whisker box plots displaying median, lower and upper quartiles, and whiskers representing minimum and maximum of the data.

Figure S3 - Ren et al.



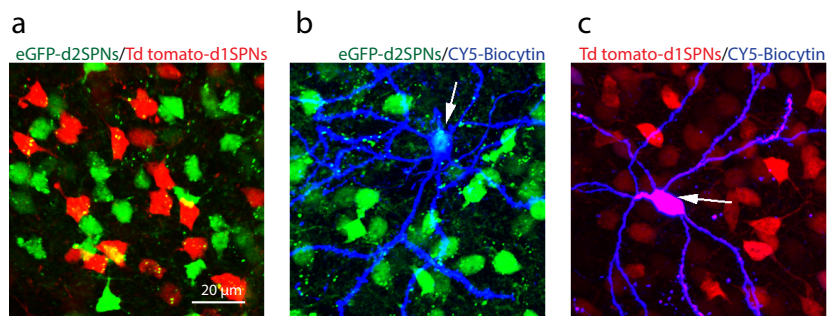
**Figure S3.** In open field test, chemogenetic activation of cNac d2SPNs in PSAM-5HT3 expressing SNI mice by PSEM89S treatment unchanged locomotor activities ( $U = 17$ ,  $p = 0.9773$  for Sham versus Saline-SNI;  $U = 19$ ,  $p = 0.9433$  for Saline-SNI versus PSEM-SNI). Data are reported as median, first and third quartiles (box plots), and minimum and maximum of data set (whiskers), and are analyzed by Mann-Whitney test.

Figure S4 - Ren et al.



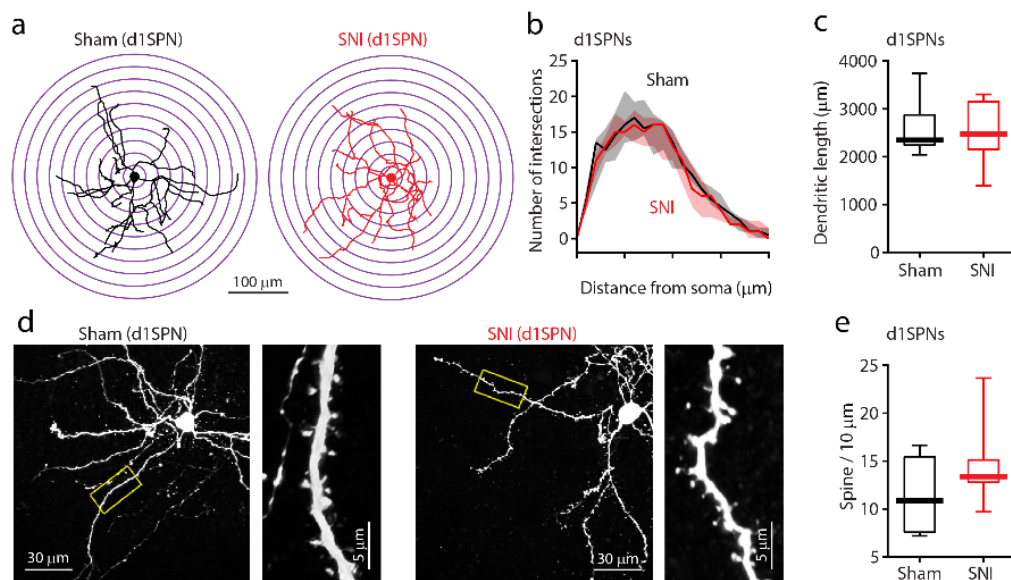
**Figure S4. a**, The Chemogenetic inhibition of cNac projection VTA neurons by intraperitoneal injections of PSEM in RV-Cre (in cNac) and AAV-PSAM-GlyR (VTA) viruses infected mice had no effect on SNI-induced tactile allodynia ( $n = 6$  for each group;  $U = 15.50$ ,  $p = 0.7359$ ). **b**, activation msNac projecting VTA neurons by the same virus strategy unchanged the social recognition deficits in SNI mice ( $n = 5$  in control and  $n = 6$  in PSEM;  $U = 20$ ,  $p = 0.2159$ ). Data are reported as median, first and third quartiles (box plots), and minimum and maximum of data set (whiskers), and are analyzed by Mann-Whitney test.

Figure S5 - Ren et al.



**Figure S5. Biocytin visualized the SPNs' dendritic morphology in the cNac slices from Christmas (Xmas) transgenic mice. *a***, The d2SPNs (eGFP-positive, green) and d1SPNs (Td tomato-positive, red) are identified in the same cNac slice taken from BAC transgenic mouse (Calibration: 20 μm). ***b***, The biocytin-filled neuron overlapped with populations of d2SPNs. ***c***, Another biocytin-filled neuron overlapped with populations of d1SPNs.

Figure S6 - Ren et al.



**Figure S6. Morphological analysis in reconstructed d1SPNs from SNI and Sham animals. a-c,** For d1SPNs, no significant difference in Sholl analysis or total tree length was detected between SNI and Sham ( $n = 8$  from 5 mice in each group,  $U = 13639$  and  $p = 0.5946$  for **b** and  $U = 31$  and  $p = 0.9319$  for **c**, Mann-Whitney test). **d:** Representative images of d1SPN dendrites/spines from SNI/Sham animals. **e,** Spine density of d1SPNs were similar between SNI and Sham ( $n = 8$  from 5 mice in each group, Mann-Whitney test with  $U = 21$ ,  $p = 0.2747$ ). Data for **b** are shown as median with shaded interquartile (quartile 1 to quartile 3); whisker box plots are displayed as median, lower and upper quartiles, and whiskers representing minimum and maximum of the data.